Memoirs of the Faculty of Engineering, Kyushu University, Vol.66, No.2, June 2006

3-D MAM Inversion in Sibayak Geothermal Field, Indonesia

by

Supriyanto SUPARNO*, Hideki MIZUNAGA** and Keisuke USHIJIMA***

(Received May 7, 2006)

Abstract

Sibayak geothermal field is located about 65 km to the southwest of Medan in the North Sumatra Province, Indonesia. Starting from 1998, a small-scale geothermal power plant (2 MWe) has been installed in this area. Since electricity demand increases in the North Sumatra Province, Pertamina Geothermal Energy plans to increase the capacity to 20 MWe. Accordingly, detailed knowledge of the reservoir structure and its extension must be determined for a new production target. The mise-a-la-masse (MAM) surveys were carried out in this field using the exploration well SBY-1 and the production well SBY-4 to delineate a new production target for further field development. A conventional one-dimensional MAM data processing has been done to obtain lateral variation of subsurface resistivity. However, the result is not satisfied to image real condition of the geology on the subsurface. Therefore, we carried out an advanced 3-D MAM inversion based on the smoothness-constrained least-squares method using a homogeneous earth as the simplest assumption of the starting model. Interpretation of the 3-D MAM model was done by combining the results with previous geo-electrical data and borehole information to image a promising reservoir zone. The resistivity model obtained from this study is characterized by a very low resistivity cap rock beneath a resistive layer and rather high resistivity layer of the reservoir. The very low resistivity layer is due to clay minerals such as montmorillonite. This interpretation result of the 3-D MAM model indicates that reservoir zones trend to the north-northeast direction of the study area, between Mt. Sibayak and Mt. Pratektekan, and shows a good correlation with the formation temperature and the lost circulation zone. This geophysical information is useful for the task of selecting sites for the promising zone in the Sibayak geothermal field.

Keywords: 3-D inversion, MAM, Geothermal, Sibayak field, Indonesia

* Graduate Student, Department of Earth Resources Engineering
** Associate Professor, Department of Earth Resources Engineering
*** Professor, Department of Earth Resources Engineering

1. Introduction

The Sibayak geothermal field is the first developed geothermal field in the Sumatra Island, Indonesia. **Figure. 1** shows the map of Sibayak field location in the North Sumatera province. The field is situated in high topography area at an elevation of between 1400 and 2200 m above sea level. Sibayak field has a liquid-dominated geothermal reservoir with temperature higher than 250°C.

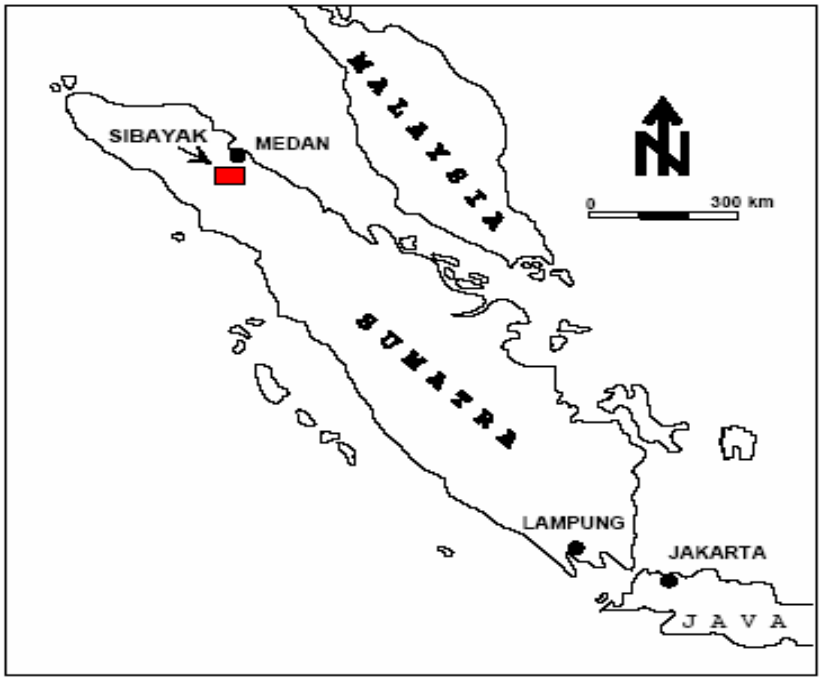

Fig. 1 Location map of Sibayak geothermal field.

The Sibayak geothermal field has been managed by PT. Pertamina, and the power generation by PLN (State Electricity Company). Starting from 1989, various geoscientific surveys have been conducted including geology, geochemistry and geophysics. The exploration result suggested that the Sibayak field has a high potential to be developed. In order to understand the real subsurface condition of Sibayak field, Pertamina Geothermal Energy has drilled 10 wells (i.e., SBY-1 to SBY-10) to depths ranging from 1500 - 2200 m. Currently it has 2 MWe installed capacity. However, due to increasing electricity demand in the province, the field is being projected to produce 20 MWe. Therefore, a better understanding of Sibayak geothermal system is required.

To obtain this achievement, we used resistivity data obtained from MAM measurement for imaging subsurface structure in Sibayak geothermal field. A previous MAM data processing was done by using one-dimensional inversion technique for mapping lateral resistivity variation in the subsurface[1]. However, the resistivity distribution in vertical and horizontal directions in the subsurface have not been provided. Moreover, one-dimensional interpretation is not fully satisfactory to describe the actual three-dimensional geological structure. Therefore, for sharpening the better target for further investigation of the prospecting area, we have re-analysed and re-interpreted the MAM data by performing three-dimensional inversion in this study. This inversion technique has been previously implemented in the Sumikawa geothermal field, Japan[2].

This paper firstly describes an overview of Sibayak field. Then, a brief explanation about the inversion technique used in data processing. Finally, it is followed by the interpretation result integrated with existing geological and borehole data.

2. Field Overview

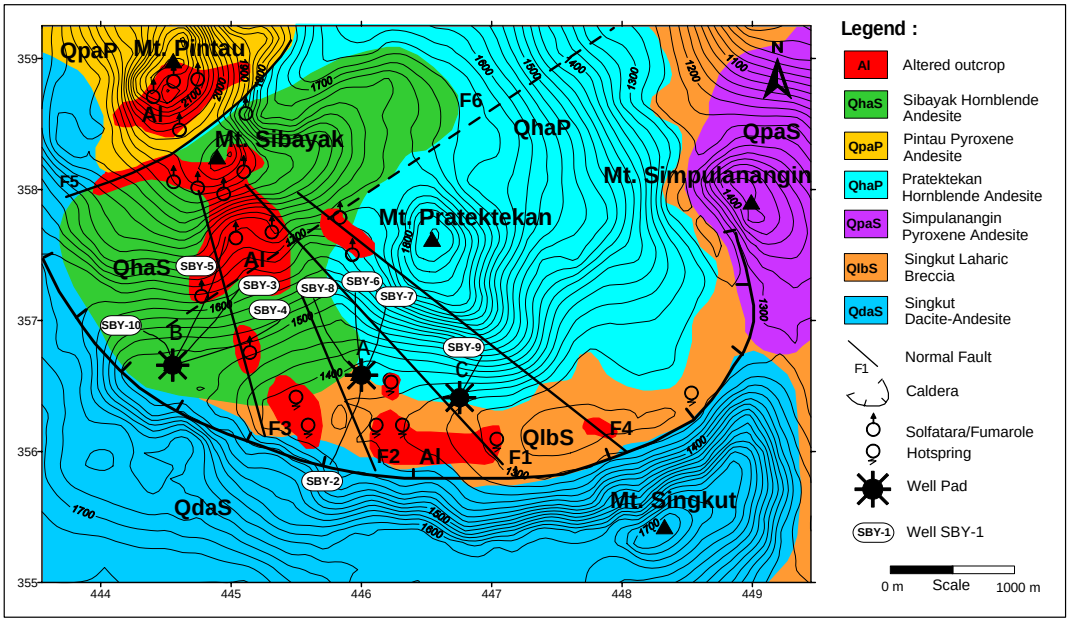

Fig. 2 Geological setting of Sibayak field.

Sibayak field is a typical volcanic geothermal system located inside the large Singkut caldera. The geologic condition and thermal manifestation of Sibayak field[3] are shown in **Fig. 2**. The field has a high topographic setting and has been a complex volcanic history in the area with a number of centers of eruptions developing over a considerable period of time within Quarternary.

A lot of geothermal manifestations such as solfataras and fumaroles are found at high elevations in the area between Mt. Sibayak and Mt. Pratektekan. The largest fumarole, indicated as up-flow zone, exists on the eastern flank of Mt. Sibayak around the center of the fracture zone. Chloride springs with silica sinter exist at lower elevations in the southern and southeastern part of Mt. Pratektekan around the Singkut caldera rim. Some fault structures within the caldera have orientation to NW-SE and extend to the center of Mt. Sibayak and Mt. Pintau. All of surface manifestations indicate that Sibayak field may be classified as high temperature geothermal system.

The volcanic rock formation is composed of andesite, andesite breccia and tuff breccia. Relatively moderate clay and chloritic hydrothermal alteration are found within this formation. Based on geological study, the sedimentary formation, as outcropped to the west and east of Mt. Sibayak and found in deeper level within the wells, is predominantly sandstone followed by shale and limestone. Drilling data show that the sedimentary formation is generally found 1150 m below the surface. The most permeable zones are encountered by the wells at deeper levels within the sediments associated with sandstone and limestone lithologies as well as along the contact of volcanic and sedimentary formations. In the area drilled to date it appears as if the geothermal reservoir is confined to these sedimentary units.

The formation temperatures in the Sibayak geothermal field were measured in the existing wells during well-completion tests. The high temperatures (**Fig. 3**), that is more than 250°C at depth -300 m asl, occurs to the north beneath Mt. Sibayak and to the northeast beneath Mt. Pratektekan. The highest temperature zone (about 280°C) was observed beneath the eastern flank of Mt. Sibayak near the largest fumarole location.

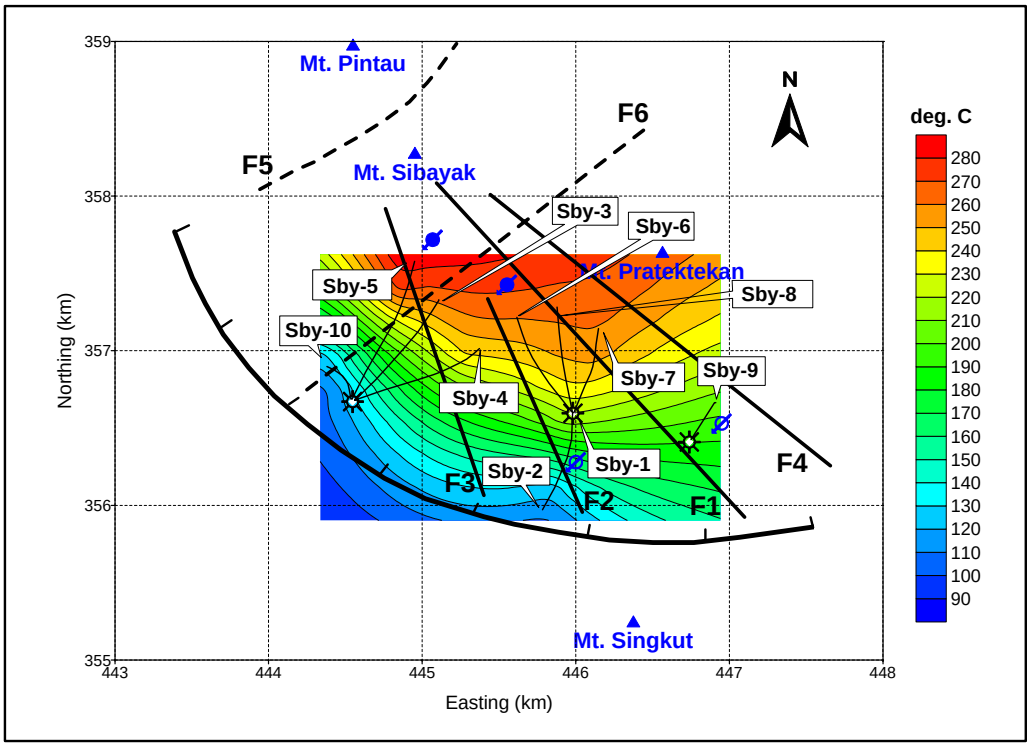

Fig. 3 Distribution of the formation temperatures at the elevation of -300 m asl.

The locations of fracture zones were identified by the occurrence of lost circulation zones encountered during drilling completion. High-lost circulation zones were found in all of existing wells at various of depths. Based on this fact, as shown in **Fig. 4**, the permeability distribution consist of three zones[4]. The high permeability area (Kh = 2-4 D.m) is located in the area between Mt. Sibayak and Mt. Pratektekan where many geothermal manifestations are found. Meanwhile, the low permeability (Kh = 0.5 D.m) is widely distributed near the Singkut caldera rim.

3. MAM Resistivity Measurement

The electrodes arrangement of the MAM equipments applied in the geothermal field are shown in **Fig. 5**. In the Sibayak geothermal field, the measurements were conducted using the wells SBY-1 and SBY-4 covering almost about 12 km^2 area. **Figure. 6** shows the layout of the field measurement, where measurement were performed along 14 survey lines (163 points) around the well SBY-1, while around the well SBY-4, the measurements were done along 12 survey lines (148 points). The survey line could not be made in the same length due to field conditions. The main target of measurement was to obtain apparent resistivity values derived from the measured potential difference between P1 and P2.

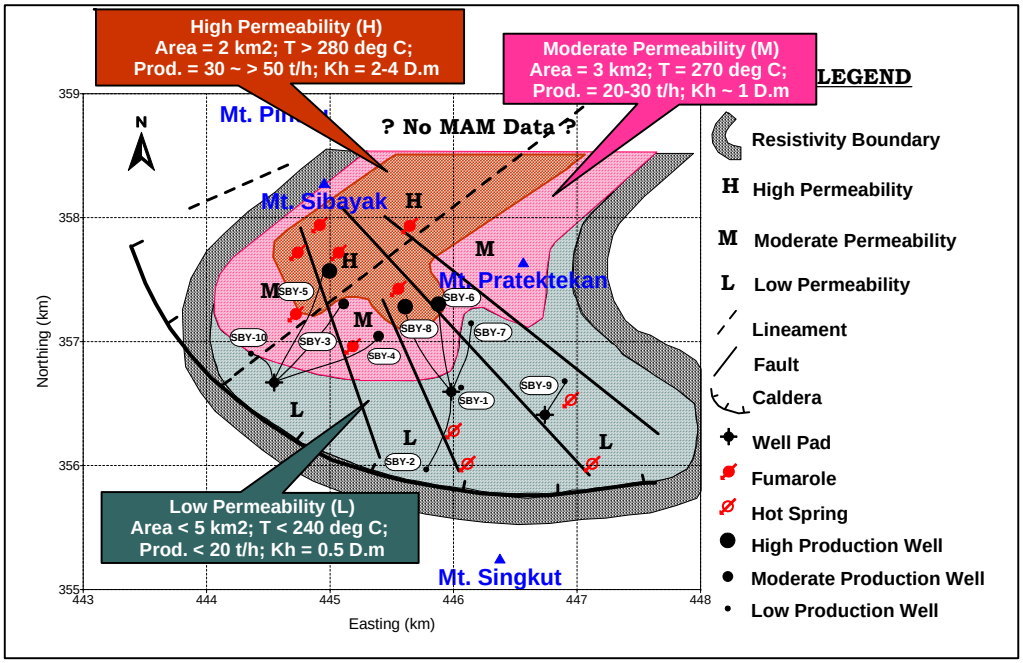

Fig. 4 Permeability distribution map of the Sibayak geothermal field.

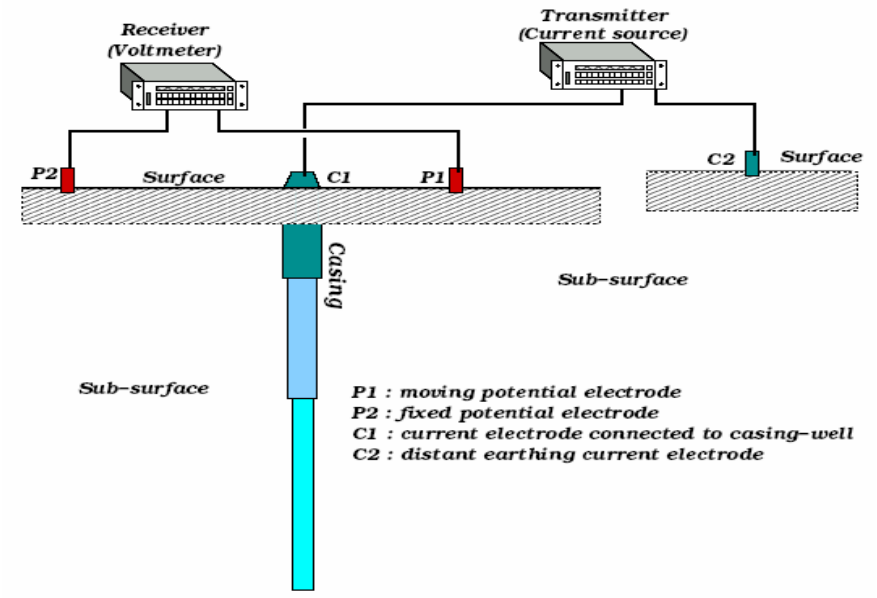

Fig. 5 Electrodes configuration in the MAM resistivity survey.

Kauahikaua introduced a potential difference formula between P1 and P2 caused by line-source electrode[5]. The formula is expressed as:

$$\phi = \frac{\rho I}{2\pi\ell} \ln\left(\frac{\ell + \sqrt{\ell^2 + r^2}}{r}\right) \tag{1}$$

where ϕ, ρ, I, ℓ, and r are the potential difference, the resistivity, the electric current, the length of the line electrode (well casing), and the horizontal distance, respectively. The horizontal distance is measured from the well (C1) at which the potential is measured (P1). Actually, during the field survey, we used two potential electrodes P1 and P2 to make a close-loop of current flowing within the subsurface. Therefore, a formulation of the potential difference between the two potential electrodes derived from Equation (1) is expressed as,

$$\Delta\phi_{12} = \frac{\rho I}{2\pi}\left\{\frac{1}{\ell}\ln\left(\frac{\overline{P_2C_1}\left(\ell+\sqrt{\ell^2+\overline{P_1C_1}^2}\right)}{\overline{P_1C_1}\left(\ell+\sqrt{\ell^2+\overline{P_2C_1}^2}\right)}\right)-\frac{1}{\overline{P_1C_2}}+\frac{1}{\overline{P_2C_2}}\right\} \tag{2}$$

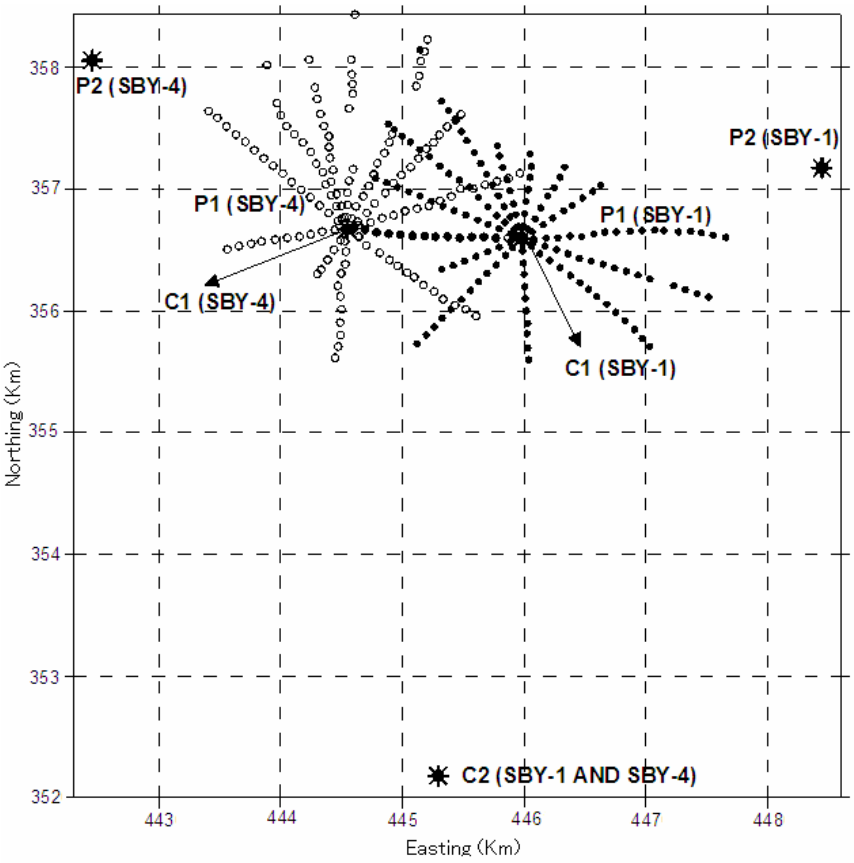

Fig. 6 Layout of electrodes arrangement for MAM measurement in Sibayak field.

4. Three-Dimensional Inversion

In order to image subsurface resistivity distribution in the vertical and horizontal directions, which is associated with fracture zones and their extensions near production wells, an attempt has been performed by using the 3-D inversion of the borehole-to-surface resistivity data.

In general, the resistivity inverse problem can be expressed as:

$$\Delta \boldsymbol{d} = \boldsymbol{A}\Delta \boldsymbol{p} \tag{3}$$

where $\Delta \boldsymbol{d}$ is the vector of differences between modeled responses and data, $\Delta \boldsymbol{p}$ is the correction vector to the initial model parameters $\boldsymbol{p}_o$, and $\boldsymbol{A}$ is a Jacobian matrix. A common approach for the model parameterization is to divide the model into rectangular blocks of unknown constant resistivity as shown in **Fig. 7**. The smoothness-constrained least-squares method can be used to determine the resistivity of the rectangular blocks (the model parameters) that will minimize the differences between the calculated and measured apparent resistivity values[6]. The least square equation used is:

$$(\boldsymbol{A}^T \boldsymbol{A} + \lambda \boldsymbol{C}^T \boldsymbol{C})\Delta \boldsymbol{p} = \boldsymbol{A}^T \Delta \boldsymbol{d} \tag{4}$$

where λ is the damping factor, $\Delta \boldsymbol{d}$ is the discrepancy vector containing the logarithmic differences between the measured and calculated apparent resistivity values, and $\Delta \boldsymbol{p}$ is the correction vector to the model parameters. The effect of the 3-D flatness filter $\boldsymbol{C}$ is to constrain the smoothness of the model parameters to some constant values. The logarithms of the model resistivity values are used in the calculation of the model correction vector $\Delta \boldsymbol{p}$.

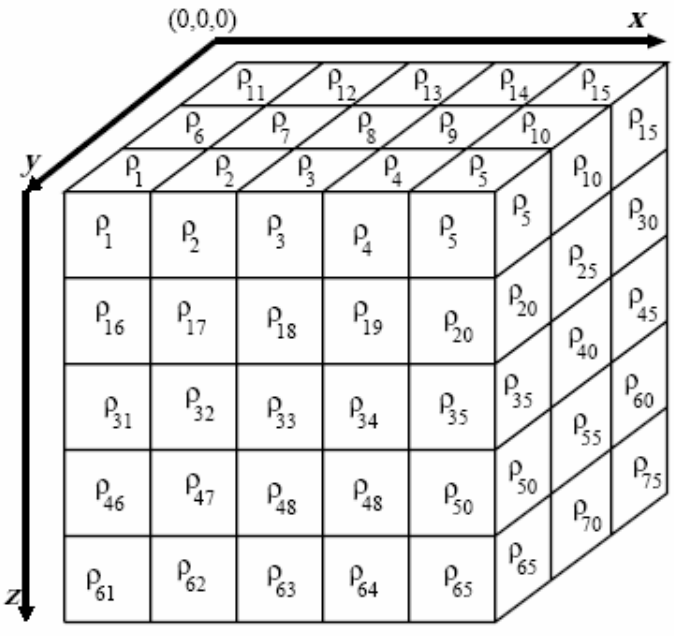

Fig. 7 Blocks of resistivity for 3-D inversion.

The next important step is to determine the partial derivative values or Jacobian matrix $\boldsymbol{A}$ for this model. McGillivray has discussed various numerical and analytical techniques for determining the partial derivatives, particularly for geoelectrical problems[7]. For the homogeneous earth model, it is possible to determine the partial derivatives analytically by using the analitic solutions of the

potential and the Green's function. For a homogeneous half-space with resistivity ρ, Poisson's equation is given by

$$\nabla^2\phi = -\rho \boldsymbol{I}_s \delta(\boldsymbol{x}_s) \tag{5}$$

where ϕ is the potential resulting from a point-current source I_s located at x_s. Meanwhile, it is well-known that for calculating the elements of Jacobian matrix, we require a big space of memory and long processing time. Therefore, in order to minimize processing time and memory, the Jacobian matrix proposed by Park and Van[8] is used. The Jacobian formulation is written by

$$A_{ij} = \left(\frac{\rho_j}{\phi_i}\right)\frac{\partial \phi_i}{\partial \rho_j} \tag{6}$$

where i is number of observed data and j is number of blocks. By carrying out a perturbation of the above equation, it can be shown that the change in the potential $\delta\phi$, resulting from a change in the subsurface resistivity $\delta\rho$ is given by

$$\frac{\partial \phi}{\partial \rho} = \rho^{-2}\int_V \nabla\phi\nabla\phi' d\tau \tag{7}$$

It is assumed that the change in the resistivity has a constant value in a volume element V and is zero elsewhere. The parameter ϕ' is the potential resulting from a "ficticious" unit current source at the potential electrode location. The homogeneous earth as the simplest assumption of the starting model[9] has been implemented in the Equation (7). Therefore, under the assumption, the initial resistivity in each block becomes the same value. By this assumption, the partial derivative can be calculated analytically by using the analytic solutions of the potential and the Green's function.

In case of a point source of current (**Fig. 8**), the partial derivative of the potential ϕ due to a change in resistivity of a volume element V in a homogeneous half-space with resistivity ρ is given by:

$$\frac{\partial \phi}{\partial \rho} = \frac{I}{8\pi^2}\int_{z_1}^{z_2}\int_{y_1}^{y_2}\int_{x_1}^{x_2}(P+Q)dxdydz \tag{8}$$

$$P = \frac{(x-x_c)(x-x_p)+(y-y_c)(y-y_p)+(z-z_c)z}{\left[(x-x_c)^2+(y-y_c)^2+(z-z_c)^2\right]^{3/2}\left[(x-x_p)^2+(y-y_p)^2+z^2\right]^{3/2}}$$

$$\boldsymbol{Q} = \frac{(\boldsymbol{x}-\boldsymbol{x_c})(\boldsymbol{x}-\boldsymbol{x_p})+(\boldsymbol{y}-\boldsymbol{y_c})(\boldsymbol{y}-\boldsymbol{y_p})+(\boldsymbol{z}+\boldsymbol{z_c})\boldsymbol{z}}{\left[(\boldsymbol{x}-\boldsymbol{x_c})^2+(\boldsymbol{y}-\boldsymbol{y_c})^2+(\boldsymbol{z}+\boldsymbol{z_c})^2\right]^{3/2}\left[(\boldsymbol{x}-\boldsymbol{x_p})^2+(\boldsymbol{y}-\boldsymbol{y_p})^2+\boldsymbol{z}^2\right]^{3/2}}$$

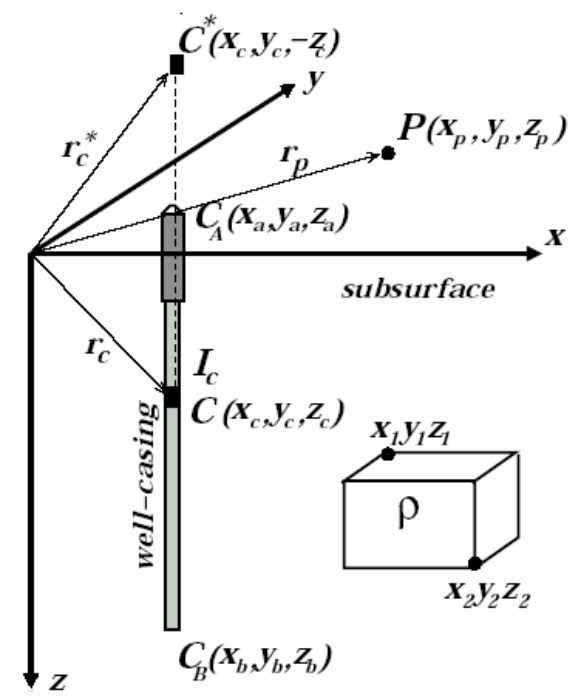

Fig. 8 The geometry of 3-D model of a block.

where *C* and *P* denote the current and potential electrode, respectively.

In case of line-source of current, Equation (8) needs to be modified by integrating process along the length of well casing. If we assume that a point-source of current C moves from well-anchor $C_A(x_A,y_A,z_A)$ to well-bottom $C_B(x_B,y_B,z_B)$ along the length of the well as a line-source of current, the point-source position $C(x_C,y_C,z_C)$ can be expressed using a parameter t ($-1 < t < 1$) as:

$$\begin{aligned} x_c &= \left[(x_A - x_B)t + x_A + x_B\right]/2 \\ y_c &= \left[(y_A - y_B)t + y_A + y_B\right]/2 \\ z_c &= \left[(z_A - z_B)t + z_A + z_B\right]/2 \end{aligned} \tag{9}$$

Assuming current density of a line source is constant, current dI for a small element dt is:

$$dI = \frac{I}{\ell}\sqrt{dx_c^2 + dy_c^2 + dz_c^2} = \frac{1}{2}dt \tag{10}$$

Finally, this result can be substituted to Equation (8) as:

$$\frac{\partial \phi}{\partial \rho} = \frac{I}{8\pi^2} \int_{-1}^{1} \int_{z_1}^{z_2} \int_{y_1}^{y_2} \int_{x_1}^{x_2} F(x, y, z, t) dx dy dz dt \tag{11}$$

The above volume integral can be evaluated numerically by using Gaussian quadrature for multiple integral.

As a conclusion, the inversion method generally may be divided into three main steps. The first step is to obtain the measured apparent resistivity by using Equation (1). The second step is to calculate the Jacobian matrix $\boldsymbol{A}$ of partial derivatives. The third step is to solve the system of linear equations in the Equation (3).

5. Data Processing and Interpretation

5.1. One-dimensional result

Before entering the main discussion of three-dimensional inversion result, we noticed some important points from the previous work as a result of residual resistivity distribution derived from one-dimensional inversion of MAM data[9].

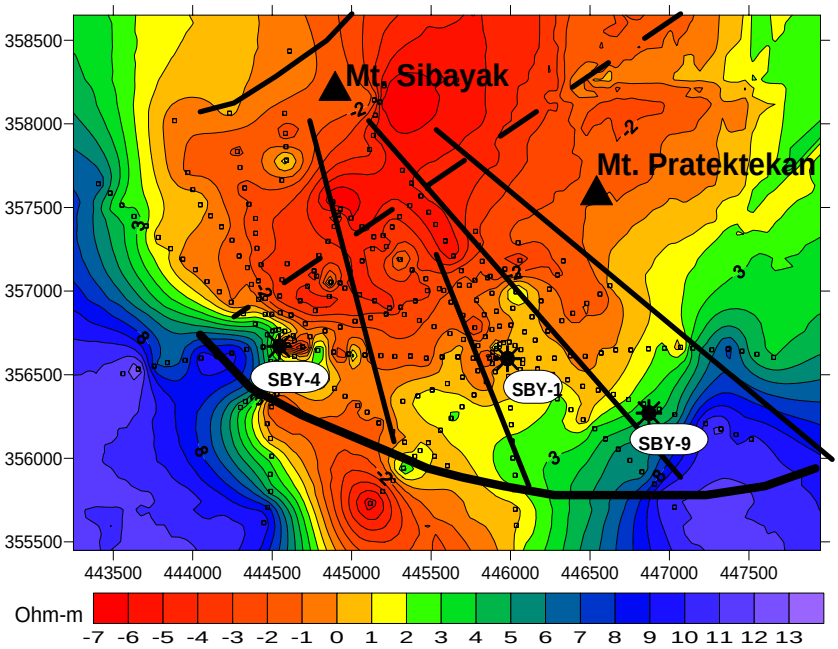

Fig. 9 Residual resistivity distribution of the Sibayak geothermal field derived from the MAM measurements.

The residual resistivity values are calculated by the inversion MAM program using the two layer earth model in each of the wells SBY-1 and SBY-4. **Figure. 9** shows a map of compilation of residual resistivity distribution from the wells SBY-1 and SBY-4 ranging from -7 to 13 Ωm. By careful inspection to the map, it is obviously recognized that the negative residual resistivity anomaly zone (less than -2 Ωm) is mainly located inside the Singkut caldera, except a small area in the southern part of the area. It could be inferred that the main reservoir may exist at the northwest of the well SBY-1 or at the northeast of the well SBY-4. Moreover, the shape of the negative anomaly coincides with the faulting system. Therefore, the lost circulation zones around the wells

SBY-1 and SBY-4 are probably reflected by the NW-SE trending faults. The fault structures may control the high permeability in the Sibayak area. In addition, another anomaly of low residual resistivity is recognized at the southern part of the Sibayak area, and may be interpreted as a permeable zone outside the Singkut caldera margin, which may have a connection to the main reservoir.

5.2 Three-dimensional result

The 3-D inversion analysis was performed using a 3-D inversion program based on the least squares algorithm written by Fortran. In this analysis, the subsurface is divided into 8 layers, whereas number of block is about 33x23x9. The results are displayed in **Fig. 10** and **Fig. 11**.

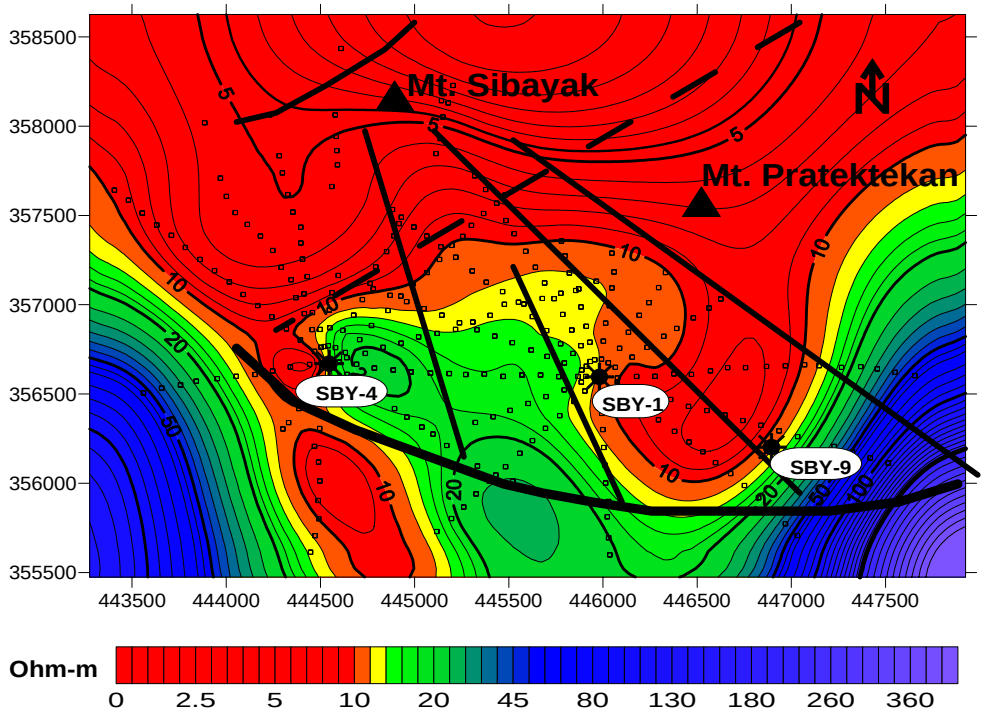

Fig. 10 Resistivity contour map of the first layer with depth between 0 – 250 m.

In a shallow depth down to 250 m, high resistivity zones, that is more than 50 Ωm, exist in the southwest and southeast directions of Sibayak field. These zones are interpreted by fresh volcanic rock zones where no geothermal manifestations are discovered on these zones. In contrast, the strongly altered rock zone indicated by low resistivity (less than 10 Ωm) is distributed in the northern part of the well SBY-4 around Mt. Sibayak where many fumaroles are found. By careful inspection to the map, it is estimated that the low resistivity zone in the northern part of the well SBY-4 follows the NE-SW lineament (F6) encountered between Mt Sibayak and Mt Pratektekan.

In the southern part of the well SBY-4 across the Singkut caldera rim, a smaller zone of the low resistivity may be caused by extending the altered cap rock zone surrounding the caldera structure. This result is quite interesting because there are no thermal manifestations on the surface. Meanwhile, the variation of formation temperature with depth obtained from the nearest well to the zone (SBY-10) suggested that the conduction thermal activity occur below the zone. On the other hand, in the north direction of the well SBY-1, there is a big area of low resistivity. Unfortunately,

because no potential electrodes are available in this area, no interpretation could be made. In general, **Fig. 9** shows that the low resistivity zone is widely distributed inside the Singkut caldera except a small area in south direction of the well SBY-4.

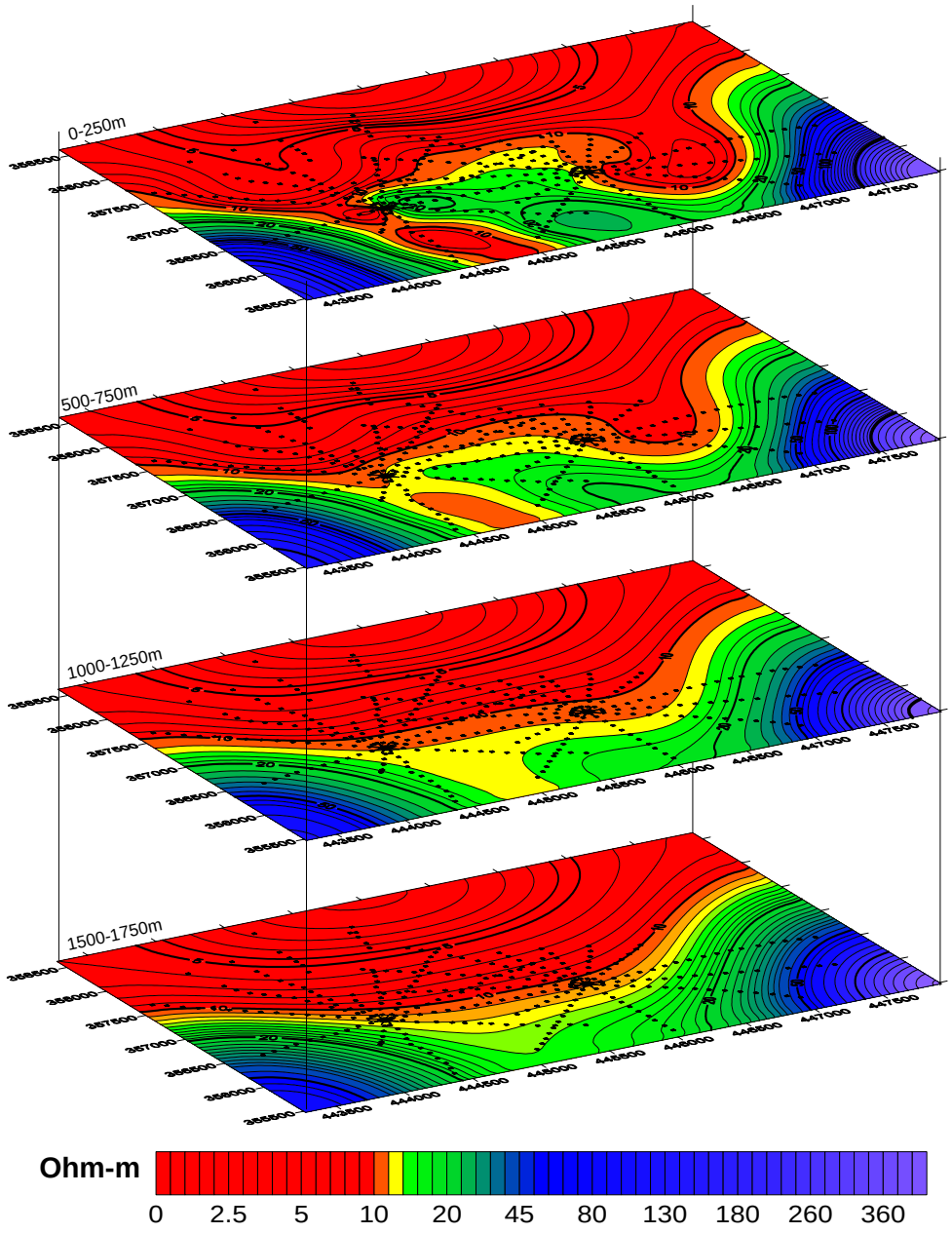

Fig. 11 Depth sliced resistivity contour map in Sibayak geothermal field.

The depth sliced resistivity contour maps ranging from 0 to 450 Ωm are shown in **Fig. 11**. In these contour maps, the highest resistivity zones (fresh volcanic rock) stay outside the caldera in the southeast and southwest direction of the Sibayak field. By comparing all depth sliced contour maps in **Fig. 11**, it is recognized that the low resistivity zone interpreted as altered cap rock formation surrounding the well SBY-4 outside the caldera has a thickness around 1 km depth. The low resistivity zone in southern part of well SBY-4 disappears more rapidly in vertical direction

than in horizontal direction. In addition, borehole information confirms that a temperature formation at depth from 0.4 to 1 km in the well SBY-10 is relatively constant around 80^{o}C. This fact can be interpreted that the rock alteration zone in this area may be caused by convective heat transfer in a fracture zone, which extends through the caldera margin to southern part of well SBY-10. The low resistivity may be caused by clay mineral as a product of alteration process.

The most interesting result is located on the eastern sector of the well SBY-1, where the low resistivity zone exists on the upper part with area around 4 km^2. The low resistivity may be interpreted as a large intense altered cap rock layer covering the geothermal reservoir. This interpretation is supported by the temperature profile obtained from the well SBY-7 which confirms that 1 km below the surface, the temperature remains constant around 260^{o}C. It can be inferred that starting from that depth, the convective heat transfer plays the main contributing factor as geothermal reservoir. In this area the resistivity model is characterized by a very low resistivity cap rock beneath a resistive layer and rather high resistivity layer of the reservoir. The very low resistivity layer is due to clay minerals such as montmorillonite.

The lowest resistivity zone in all the maps in **Fig. 11**, which can be inferred as an intense altered zone located in the center area of faulting systems between Mt. Sibayak and Mt. Pratektekan. By comparing the low resisitivity zone on **Fig. 11** and the permeability map on **Fig. 4**, we can see that the lowest resistivity zone exists almost in the same position with the highest permeability zone. The lowest resistivity zone located on the northern part of the well SBY-1 and SBY-4 coincides with a high permeability zone (Kh = 2-4 D.m). In contrast, a low permeability zone (Kh = 0.5 D.m) where encountered in vicinity of caldera margin has a high resistivity.

The resistivity contour map at the depth from 1500 m to 1750 m in **Fig. 11** might be used to explain a correlation between production rate and resistivity distribution. Based on the map, it is found that some higher production rates of wells (SBY-5, SBY-8 and SBY-6) are distributed in a low resistivity zone between Mt. Sibayak and Mt. Pratektekan. For example, the most productive well (SBY-5), which has vertical depth of about 1994 m, has produced 57 t/h of steam. Its well bottom is located in a low resistivity zone near Mt. Sibayak. It was followed by well SBY-8 (36 t/h of steam) and SBY-6 (33 t/h of steam), which has vertical depth of about 1993 m and 1750 m, respectively, also located in a low resistivity zone in the same area.

On the other hand, a low production rate has encountered in several wells where their bottoms are located in a high resistivity zone. The well bottom of well SBY-1 (18 t/h) at a depth of 1498 m is located in a high resistivity zone as well as well the bottom of SBY-9 (15 t/h) at the vertical depth of about 1527 m is also located in a high resistivity zone. This fact is consistent with the permeability distribution[4)].

6. Conclusion

According to MAM processing result, it is clearly found that the correlation between the shallow conductor (low resistivity) and hydrothermal alteration zones is quite evident. The extension of these conductors to the area surrounding the mapped alteration zones suggests that argillitization of the near-surface rocks contributes significantly to the high conductivities, as should be expected[10, 11)]. Even though a straightforward correlation between lithology and electrical resistivity is difficult to establish, the number of drillholes provides some evidence of a correlation

between a strongly altered rock dominated by clay minerals (montmorillonite) and the shallow conductive zone (resistivity of 5-10 ohm-m). This correlation would suggest that the influence of clay minerals resulting from hydrothermal alteration process is the main contributing factor to the enhanced conductivities as found in several geothermal fields in Indonesia[12].

This study also concludes that the trend of low resistivity zone extends to the area between Mt. Sibayak and Mt. Pratektekan where the higher permeability and temperature are observed. However, all the contour maps in **Fig. 11** show that the high resistivity zone (fresh volcanic rock) are mainly distributed in the southeast and the southwest of the Sibayak field where the permeability is low. Accordingly, it can be inferred that a future promising geothermal reservoir is located in the subsurface area between Mt. Sibayak and Mt. Pratektekan. This study also shows that the result of 3-D inversion of MAM is useful to estimate a distribution of subsurface permeability at a liquid-dominated reservoir such as Sibayak system.

Acknowledgements

The authors wish to express their gratitude to the Management of PT. Pertamina for providing the data and their permission to publish this paper. The first author gratefully acknowledges support from a postgraduate scholarship awarded by the Monbukagakusho Scholarship, Japan.

References

1) Daud, Y., Atmojo, J.P., Sudarman, S., Ushijima, K.,; Reservoir imaging of the Sibayak geothermal field, Indonesia using borehole-to-surface resistivity measurements, *21st New Zealand Geothermal Workshop* 1999, pp 139-144.
2) Aono, T., Mizunaga, H., Ushijima, K.; Imaging fracture during injection and production operations of reservoirs by a 4-D geoelectrical method, Proceedings of the 6th SEGJ International Symposium. Tokyo 2003, pp. 281-287.
3) Hasibuan, A and Ganda S.,; Geology of Sibayak – Sinabung Area, North Sumatra. Unpublished report, Exploration Division, Pertamina, 1989.
4) Daud, Y., Sudarman, S., Ushijima, K.,; Imaging reservoir permeability of the Sibayak geothermal field, Indonesia using geophysical measurements. Proceedings 21st Workshop on Geothermal Reservoir Engineering, Stanford, California. 2001, pp127-133.
5) Kauahikaua, J., Mattice, M., and Jackson, D., 1980, Mise-a-la-masse mapping of the HGP-A geothermal reservoir, Hawaii, Geothermal Resources Council, Transactions, **4,** 1980, pp 513-516.
6) Constable, S. C., Parker, R. L., and Constable, C. G.,; Occam's inversion: a practical algorithm for generating smooth models from EM sounding data, Geophys., **52**, 1987, pp 289-300.
7) McGillivray, P. R., and Oldenburg, D. W.,; Methods for calculating Frechet derivatives and sensitivities for the nonlinear inverse problem: A comparative study: Geophys. Prosp., **38**, 1990, pp 499-525.
8) Park, S.K., and Van, G.P.,; Inversion of pole-pole data for 3-D resistivity structure beneath arrays of electrodes, Geophys., **56**, 1991, pp 951- 960.
9) Loke, M.H., and Barker, R.D.,; Practical techniques for 3-D resistivity survey and data inversion, *Geophysical Prospecting,* **44**, 1996, 499-523.
10) Anderson, E., Crosby, D., Ussher, G., Bulls-eye! - Simple resistivity imaging to reliably locate the geothermal reservoir, Proceedings World Geothermal Congress 2000, pp 909-914.

11) Ussher, G., Harvey, C., Johnstone, R., Anderson, E.,; Understanding the resistivity observed in geothermal systems, Proceeding World Geothermal Congress 2000, Beppu, Japan, pp 1915-1920.
12) Sudarman, S., Pujianto, R., and Budiarjo, B.,; The Gunung Wayang-Windu geothermal area in West Java: Proceeding of Indonesian Petroleum Association (IPA) 15th Annual Convention, Jakarta, Indonesia, 1986, pp 141-153.